The 5th Joint International Conference on Multibody System Dynamics
June 24 –28, 2018, Lisbon, Portugal

Power spectrum analysis of contact forces and force moments during normal and modified gait

Carlos Rodrigues[1], Miguel Correia[2], João Abrantes[3], Jurandir Nadal[4] and Marco Benedetti[5]

[1] *Centre for Biomedical Engineering Research, INESC TEC, cmbr@inesctec.pt*
[2] *Department of Electrical and Computer Engineering, FEUP, mcorreia@fe.up.pt*
[3] *MovLab - Laboratório de Tecnologias e Interfaces, ULHT, joao.mcs.abrantes@ulusofona.pt*
[4] *PEB - Programa de Engenharia Biomédica, COPPE/UFRJ, jn@peb.ufrj.br*
[5] *PPGEE - Programa de Pós-Graduação em Engenharia Elétrica, benedetti@ufpe.br*

ABSTRACT — *This study applies power spectrum analysis to vertical ground reaction forces, lower limb (LL) vertical joint forces and flexion-extension force moments estimated from multibody dynamics for intra-subject variability assessment at different gait modes, namely stiff knee gait (SKG) and slow running (SR) in relation to normal gait (NG). Ground reaction forces were acquired with force plates and cartesian coordinates of LL joints registered with camera system at gait lab during NG, SKG and SR. Subject specific modelling is performed morphing Twente Lower Extremity Model (TLEM) to match the size and joint morphology of the stick-figure model for inverse dynamic. According to detected differences on power spectrum of contact forces and force moments that could be undetected on time domain, frequency analysis presented as a quantitative metric for continuum pattern assessment of subject specific internal and external lower limb contact actions at normal and modified gait.*

1 Introduction

On human gait people walk for lower velocities and run for higher velocities. Despite walking and running present alternated movement of the lower limbs they are different in several other aspects Due to pathology or injury subjects frequently adopt modified gait (MG) such as stiff knee gait (SKG) for lower velocities or slow running (SR) for higher velocities as an alternative to normal gait (NG) [1]. Gait and run are contact control activities where external and internal contact forces have to be controlled to assure stability and movement progression [2]. According to difficulty on direct measurement of internal joint forces and force moments under natural gait, multibody system dynamics (MBD) presents as a valuable tool for modelling and simulation estimating internal joint actions for registered movement, with the need of assessment of these joint actions [3]. Classical analysis of human gait has typically been performed on time domain using discrete measures of local or global extreme, maximum and minimum values and their corresponding time instants of occurrence. Discrete time analysis can be useful when there are clear differences between selected parameters but it does not take into account continuum pattern of the signals, with possible test conditions or subjects presenting similar discrete values but different continuum patterns [4]. On intra-subject variability assessment at different gait modes namely stiff knee gait (SKG) and slow running (SR) in relation to normal gait (NG) variation of internal estimated actions are frequently subtle with the need to consider continuum pattern variation of the signals. The purpose of this study is thus to assess power spectrum of subject specific joint contact estimated forces and force moments in relation with ground reaction forces, during SKG and SR for comparing its variation with NG at frequency domain.

Due to the interest on subject specific analysis at different gait modes and difficulty on average sample of different subjects to represent specific subject, attention was focused on case study at motion capture laboratory of an adult healthy male subject 70 kg mass and 1.86 m height during NG at comfortable auto-selected velocity, SKG with lower knee flexion and SR trial at minimum velocity to ensure time period with both feet off the ground.

1.1 Trial tests

Simultaneous recordings of ground reaction forces, skin markers attached to the lower extremity and EMG were obtained with two AMTI force plates sampling at 2000 Hz, eight camera Qualisys system at 100 Hz and Noraxon wireless system at 2000 Hz. Marker protocol used for analysis at musculoskeletal model includes right and left anterior superior iliac spines, thigh superior, knee medial, knee lateral, shank superior, ankle medial, ankle lateral and toes. sEMG was recorded for soleus medialis (SM) and tibialis anterior (TA) of the subject's right leg and normalized to dynamic maximum voluntary contraction with counter movement jump for SM and right leg swing for TA. Calibration measurements were performed for the skin markers, Fig. 1 [5], during static trial of standing reference and for sEMG during maximum voluntary contraction. Patient-specific kinematic model was scaled for dimensions of body segments and mass/ inertia properties using anatomical landmarks of static trial and subject mass and height. Although more markers were attached to the subject for motion capture session these were not considered at the applied marker protocol for analysis.

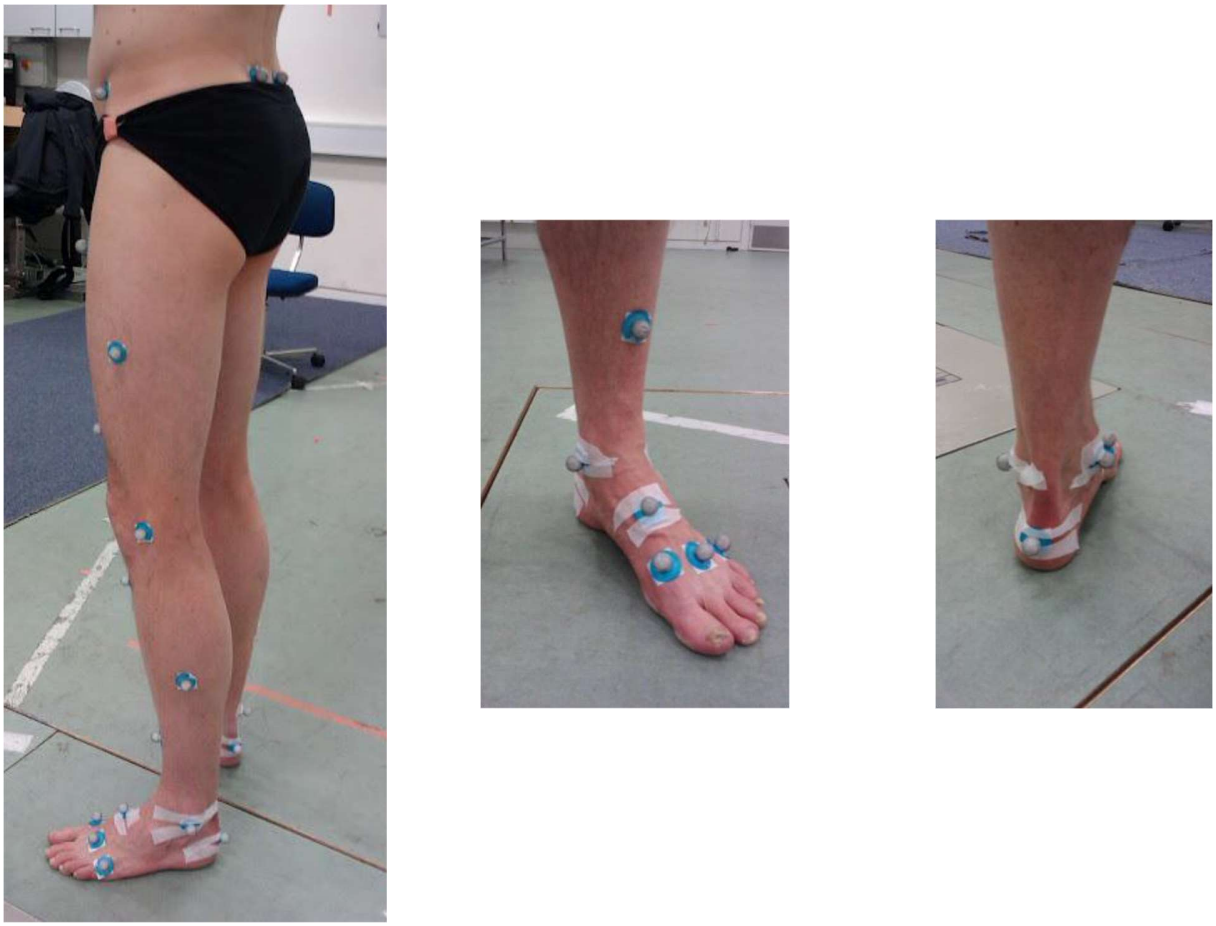

Fig. 1: Lower limb marker protocol used at trial tests, adapted [5].

1.2 Model

Applied TLEM model [6] is constituted by 8 rigid body segments with 21 degrees of freedom (DOF) including HAT (Head, Arms and Trunk), pelvis, right and left upper leg, lower leg and feet, with 3 DOF for the trunk orientation, 6 DOF for the 3D position and orientation of the pelvis, 3 DOF each for the right and left hip modeled as a ball and socket joint and 1 DOF each for the knee, ankle and subtalar joints modeled as single hinge joints. The mechanical effect of 76 muscles of both legs is implemented by 264 muscle elements described by 3D locations of its origin and insertion points on the corresponding segment, considered as independent actuators with specific muscle mass, pennation angle, physiological cross-sectional area (PCSA), tendon length and optimal fiber length. Stick-figure model was generated based on static trial and over-determinate kinematic analysis was performed over dynamic trial obtaining hip, knee and ankle joint angles, morphing TLEM [6] to match the size and joint morphology of the stick-figure model, Fig. 2, for inverse dynamic analysis based on joint angles and kinetic boundary conditions.

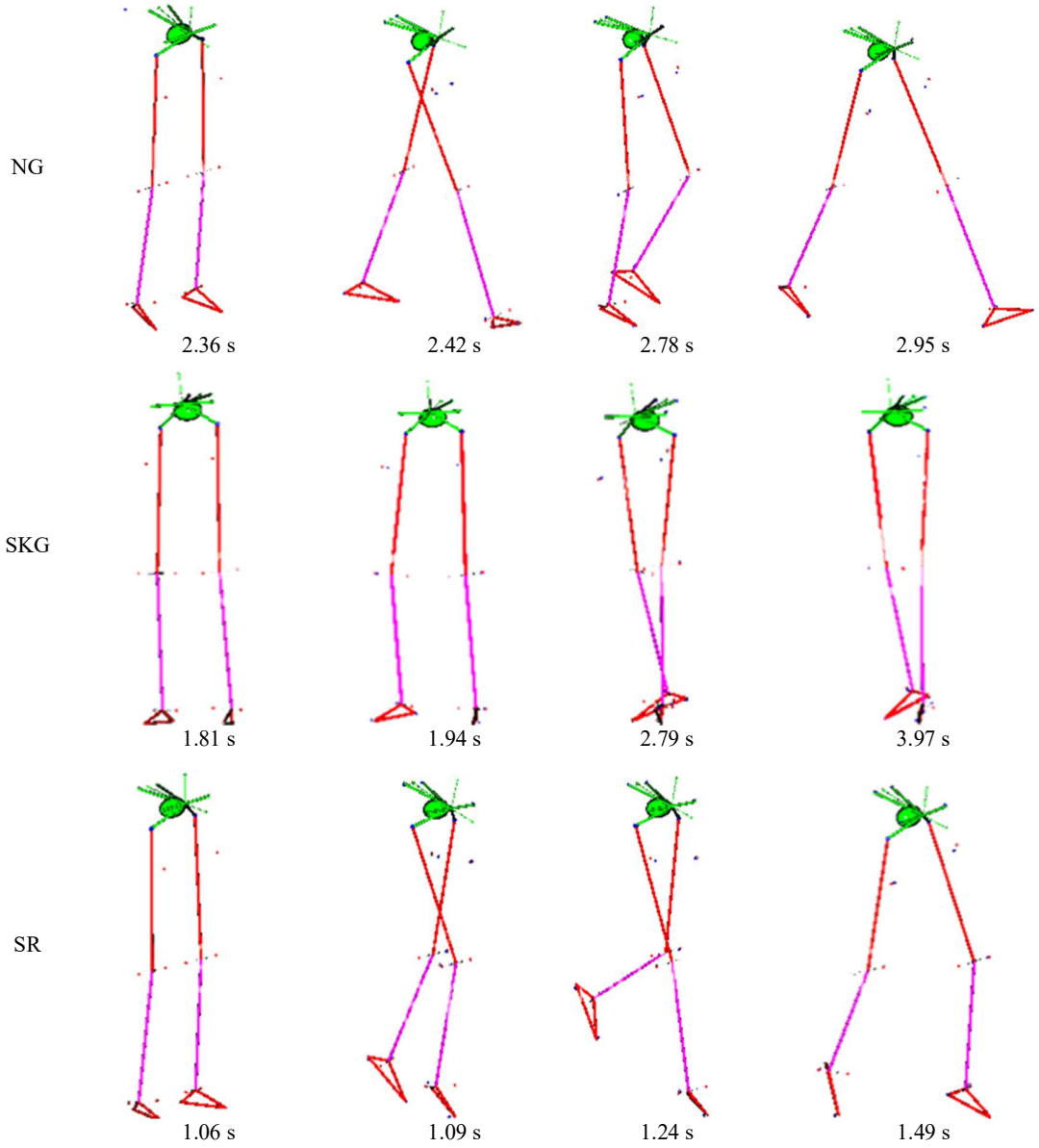

Fig. 2: Lower limb Stick figures of applied model for different phases of considered gait modes, NG, SKG and SR.

1.3 Multibody dynamics

Joint angles of the musculoskeletal model were computed from position data by inverse kinematics and joint reaction forces and force moments were computed by inverse dynamics from ground reaction forces and force moments, joint angles, angular velocities and accelerations [7], Fig.3.

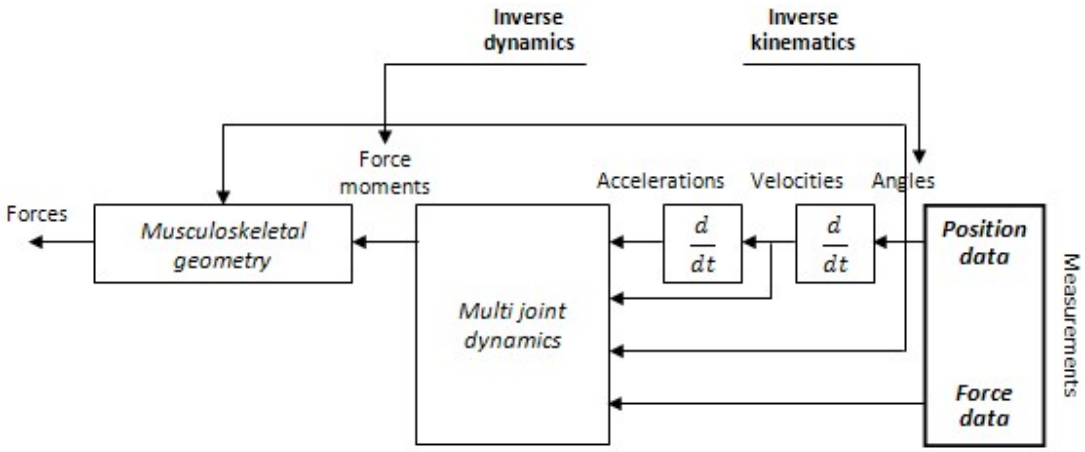

Fig. 3: Block diagram from inverse kinematics and dynamics process, adapted [7].

Due to muscle redundancy, distribution of joint forces and force moments by muscles was based on muscle grouping [3] and optimization of muscle load distribution according to min/max criterion with p=3 for synergy accounting and quadratic penalization leading to gradual increase of muscle activity with reduced contribution and limited cost of the other muscles with increased activity [8]. Hill-type musculotendon model was used for musculoskeletal simulation including three element model with serial and parallel elastic element taking into account nonlinear force-length and force-velocity properties of the contractile element [3].

1.4 Fast Fourier Analysis

Entire stride of vertical ground reaction forces (*GRFz*) as well as hip, knee and ankle joint vertical forces (*JFz*) and flexion-extension force moments (*Mfe*) were selected according to its higher amplitude for decomposition on Fourier domain with frequency of the maximum FFT coefficient amplitude assessed along with frequency of the 90th percentile of FFT relative accumulated frequency. The frequencies of the fundamental harmonics for the FFT decomposition of *GRFz*, 1.7 Hz at NG, 1.5 Hz at SKG and 3.6 Hz at SR were defined according to the time period of the right foot contact with the ground and the frequencies of the fundamental harmonics for the FFT decomposition of *JFz* and *MFe*, 0.75 Hz at NG, 0.67 Hz at SKG and 1.03 Hz at SR were defined according to the time period of the vertical joint reaction forces and the flexion-extension joint force moments for each of the considered tests.

Fourier decomposition of *GRFz*, *JFz* and *Mfe* entire stride during NG, SKG and SR represented as q_T was implemented using MATLAB R2010b (The MathWorks Inc., Natick, MA, USA) according to Eq. (1),

$$q_T^i(t) = C_0^i + \sum_{k=1}^{n_k} C_k^i \, cos\left(k\omega t + \varphi_i^k\right)$$

$$q_T^i(t) = A_0^i + \sum_{k=1}^{n_k} \left[A_k^i \cos(k\omega t) + B_k^i \, \mathrm{sen}(k\omega t)\right] \tag{1}$$

$$C_0^i = A_0^i \quad C_k^i = \sqrt{\left(A_k^i\right)^2 + \left(B_k^i\right)^2} \quad \varphi_i^k = \tan^{-1}\left(-\frac{B_k^i}{A_k^i}\right) .$$

Fourier coefficients for decomposition of *GRFz*, *JFz* and *Mfe* at Eq. (1) were obtained using Eq. (2),

$$A_0^i = \frac{1}{T}\int_0^T q_i(t)dt$$
$$A_k^i = \frac{2}{T}\int_0^T q_i(t)\cos(k\omega t)\,dt \quad (2)$$
$$B_k^i = \frac{2}{T}\int_0^T q_i(t)\,\mathrm{sen}(k\omega t)\,dt \quad ,$$

with $\omega = 2\pi/T$, T the stride period, i=1,2,3 the index corresponding to *GRFz*, *JFz*, *Mfe* and k=1,…, n_k the order of the harmonic. Fourier coefficients from *GRFz*, *JFz* and *Mfe* decomposition were analyzed according to the frequency of the harmonic with higher amplitude and 90th percentile of the Fourier series for each gait mode NG, SKG and SR. The convergence of the Fourier series was assessed according to the normalization of the partial sum expressed by Eq. (3),

$$SC(n_k) = \sum_{k=0}^{n_k} C_k^i \Big/ \sum_{k=0}^{n_k^{máx}} C_k^i$$
$$n_k^{máx} = máx\{n_k\}/2 + 1 \quad . \quad (3)$$

2 Results

A complete stride period during NG, SKG and SR was selected for analysis, corresponding to the time interval that mediates the beginning of two successive contacts of the same foot with the ground. Gait phases were time delimited at NG and SKG from vertical ground reaction forces (*GRFz*) at the start of the feet contact with the ground on initial double stance (IDS), start of the single support (SS), start of the terminal double stance (TDS), start and end of the transfer phase (TRF) and at SR at the start and end of the stance (ST), early float (EF), middle swing (MS) and late float (LF) from alternate contact of each feet with the ground, Fig. 4.

2.1 Time profiles

Time period of the gait cycle (GC) and single support (SS) *GRFz* presented higher values at SKG (1.169 s and 0.504 s) than NG (0.990 s e 0.415 s) and higher values at NG than SR (0.800 s and 0.279 s). Double support (DS) time period presented higher value at NG (0.087 s) than SKG (0.079 s) with this phase nonexistent at SR. In relation to GC, SS presents higher value at SKG (43.13%) than at NG (41.85%), with higher SS relative time period pointed as the best support index [1]. Duty factor (β) correspondent to the time fraction of the gait cycle (GC) that each foot is in contact with the floor presented higher value at NG (0.59) than SKG (0.57) and this higher value than SR (0.35) in agreement with [9]. As a result of both feet *GRFz* and time contact with the ground SKG presents higher resultant vertical impulse (686.3 Ns) than NG (584.7 Ns) and this higher value than SR (468.5 Ns). Average progression velocity assessed from pelvis antero-posterior displacement presents higher value at SR (2.5 m/s) than NG (1.8 m/s) and this higher value than SKG (1.4 m/s).

2.1.1 Vertical ground reaction forces

Vertical ground reaction forces (*GRFz*), Fig. 4, presents typical time profiles according to the contact of the foot with the ground at each gait mode, with two relative maximum and one relative minimum value at NG and SKG, as well as one absolute maximum at SR. SKG presents separate lower lateral relative maximum values of $GRFz_1(t)$ at the right (751.7 N) and $GRFz_2(t)$ at the left limbs (712.5 N) than NG (881.3 N and 777.6 N), with resultant vertical value $GRFz_{12}(t) = GRFz_1(t) + GRFz_2(t)$ presenting higher maximum values at SKG (1091.4 N)

than NG (968.5 N), both lower than SR (1577.4 N and 1493.1 N). Despite individual lateral minimum values of $GRFz_1(t)$ and $GRFz_2(t)$ occur during double support (DS) phase at NG and SKG it is at TDS that resultant maximum vertical value of $GRFz_{12}(t)$.

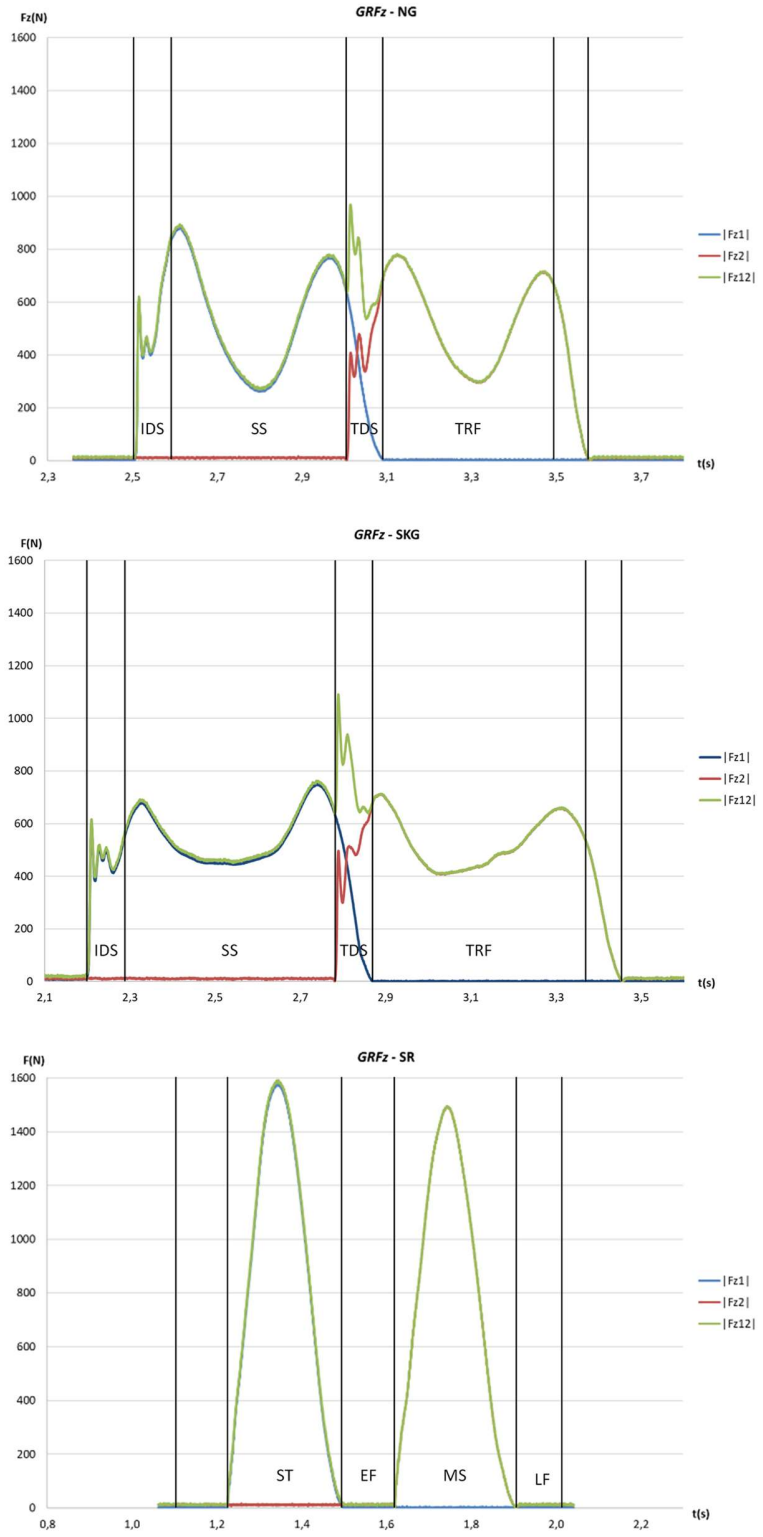

Fig. 4: Vertical ground reaction force time profile registered at the left (Fz_1), right (Fz_2) and joint (Fz_{12}) feet for NG, SKG and SR.

2.1.2 Vertical hip joint forces

Fig. 5 presents computed time profile of vertical forces at the right, left and both sides of the hip joints obtained from inverse dynamics (ID), Fig.3, during NG, SKG and SR. The hip joint vertical forces follow the characteristic of the vertical ground contact forces, with two maximum vertical values of lower magnitudes 2700 N and 4400 N for normal gait a 2400 N ripple and a 3600 N peak for stiff knee gait and a single peak value of vertical forces with higher magnitude 6500 N for slow running.

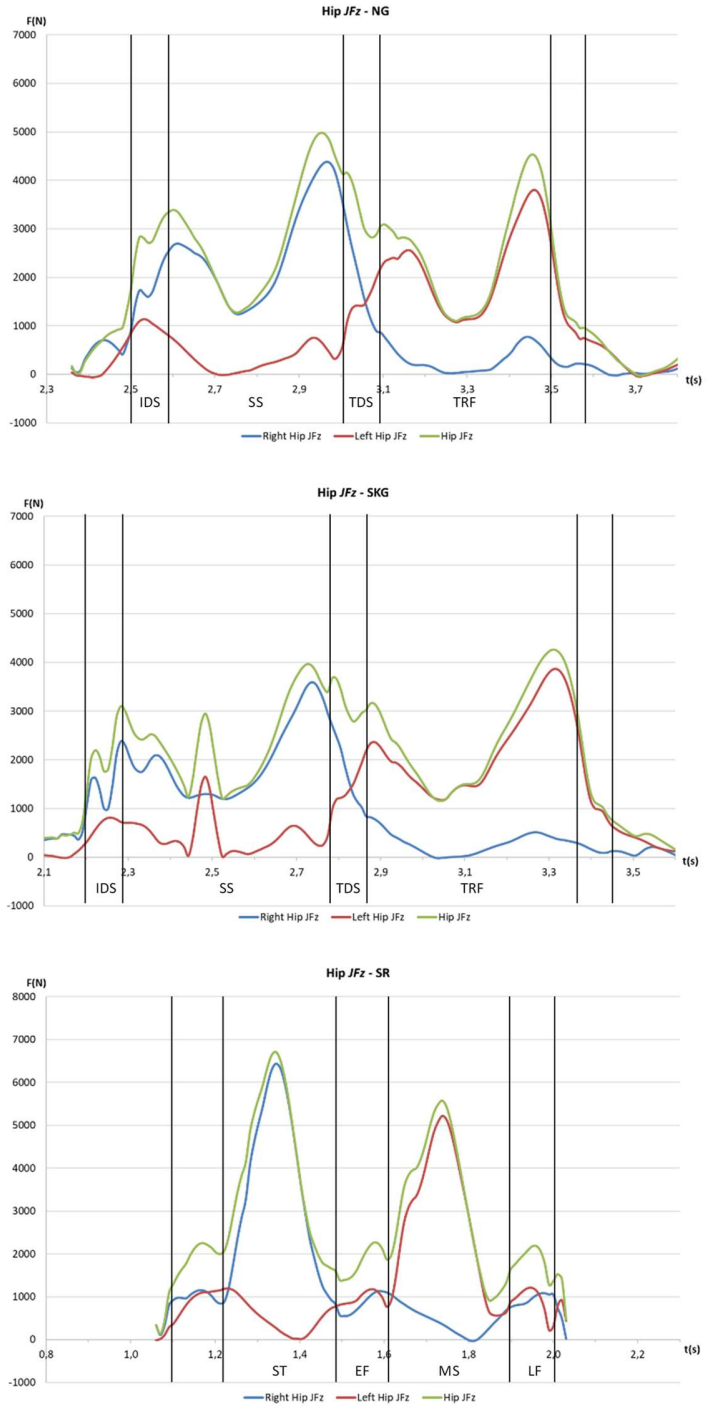

Fig. 5: Estimated time profile of vertical force at the right, left and both sides of the hip joints during NG, SKG and SR.

2.1.3 Vertical knee joint forces

Fig. 6 presents computed time profile of vertical force at the right, left and both knee joints obtained from ID, Fig.3, during NG, SKG and SR. The knee *JFz* follow the characteristic of the *GRFz*, with two maximum vertical values of lower magnitudes 3500 N and 4250 N for NG, a ripple of 1400 N and a peak at 4500 N for SKG, with a single peak value of higher magnitude 11800 N for SR. The ripple 1400 N for the SKG, fades the first peak of *GRFz* at NG approaching its profile to the SR. The value of peak force 11800 N for SR is far greater than all the other maximum *JFz* at NG and SKG.

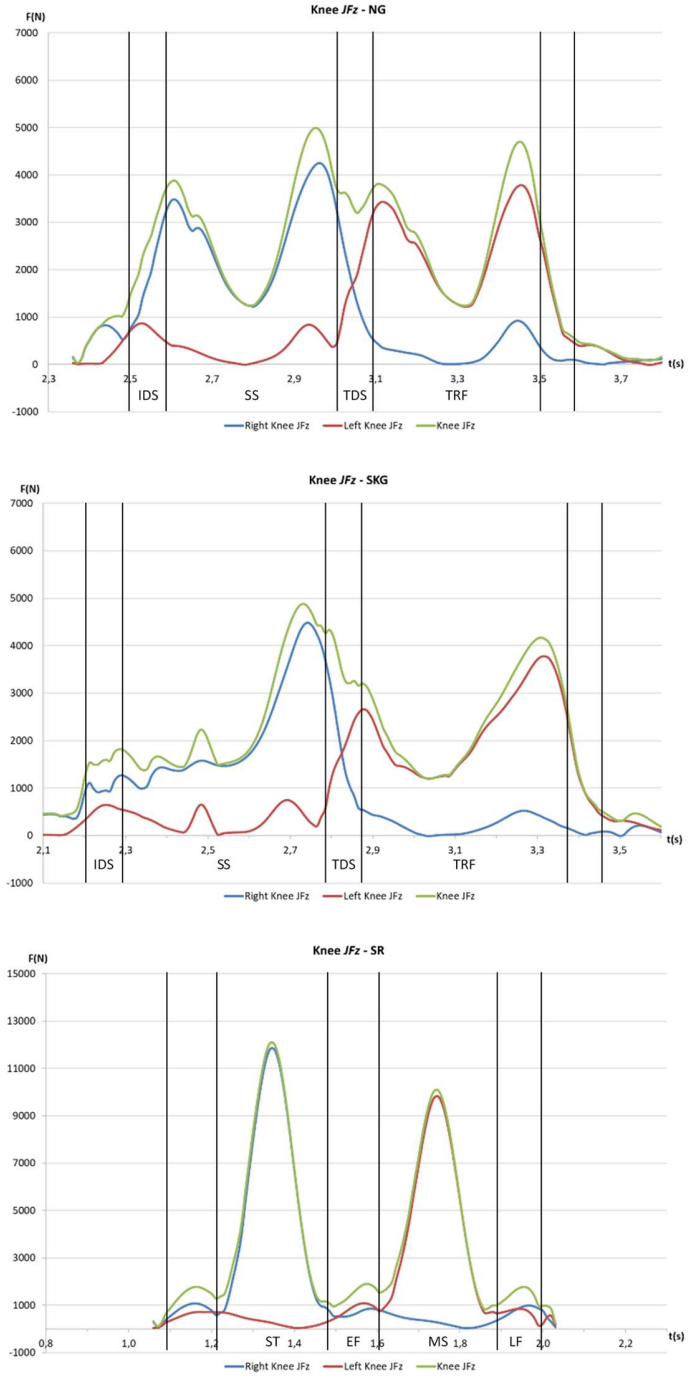

Fig. 6: Estimated time profile of vertical force at the right, left and both knee joints during NG, SKG and SR.

2.1.4 Vertical ankle joint forces

Fig. 7 presents computed time profile of vertical forces at the right, left and both ankle joints obtained from ID, Fig.3, during NG, SKG and SR. The ankle joint vertical forces present clear differences to the vertical ground contact forces, with relative maximum of lower magnitude 3000 N and an absolute maximum with higher magnitude 6100 N for NG, a subtle relative maximum with 2400 N magnitude ripple and a 6000 N peak for SKG along with a single peak value of vertical forces with higher magnitude 14500 N at the right for SR.

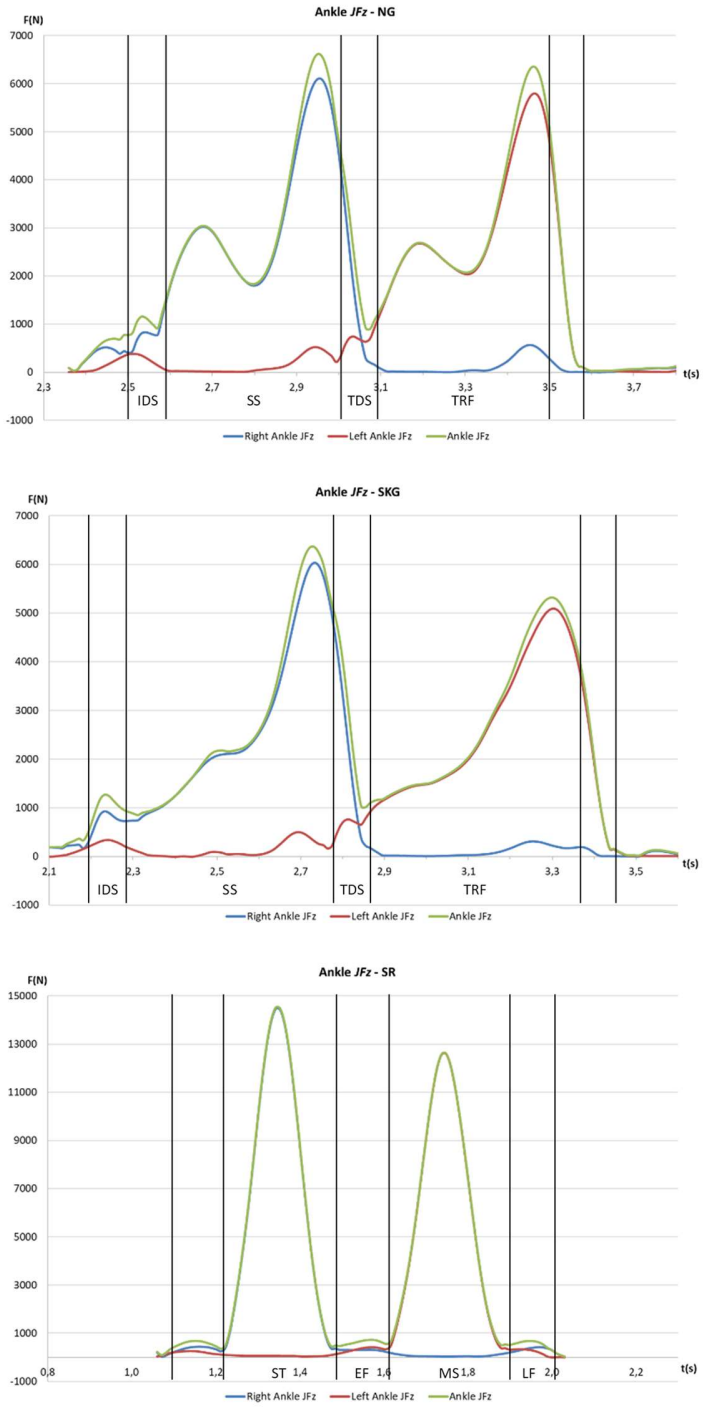

Fig. 7: Estimated time profile of vertical force at the right, left and both ankle joints during NG, SKG and SR.

2.1.5 Flexion-extension joint force moments

Slow running presents higher intensity of joint extension moments with maximum amplitude value -240 Nm for ankle plantar flexion, than gait trial with -125 Nm and stiff knee gait with -120 Nm. Hip joint flexion moments present higher values for gait trial with 78 Nm, than stiff knee gait with 71 Nm and slow running with 45 Nm.

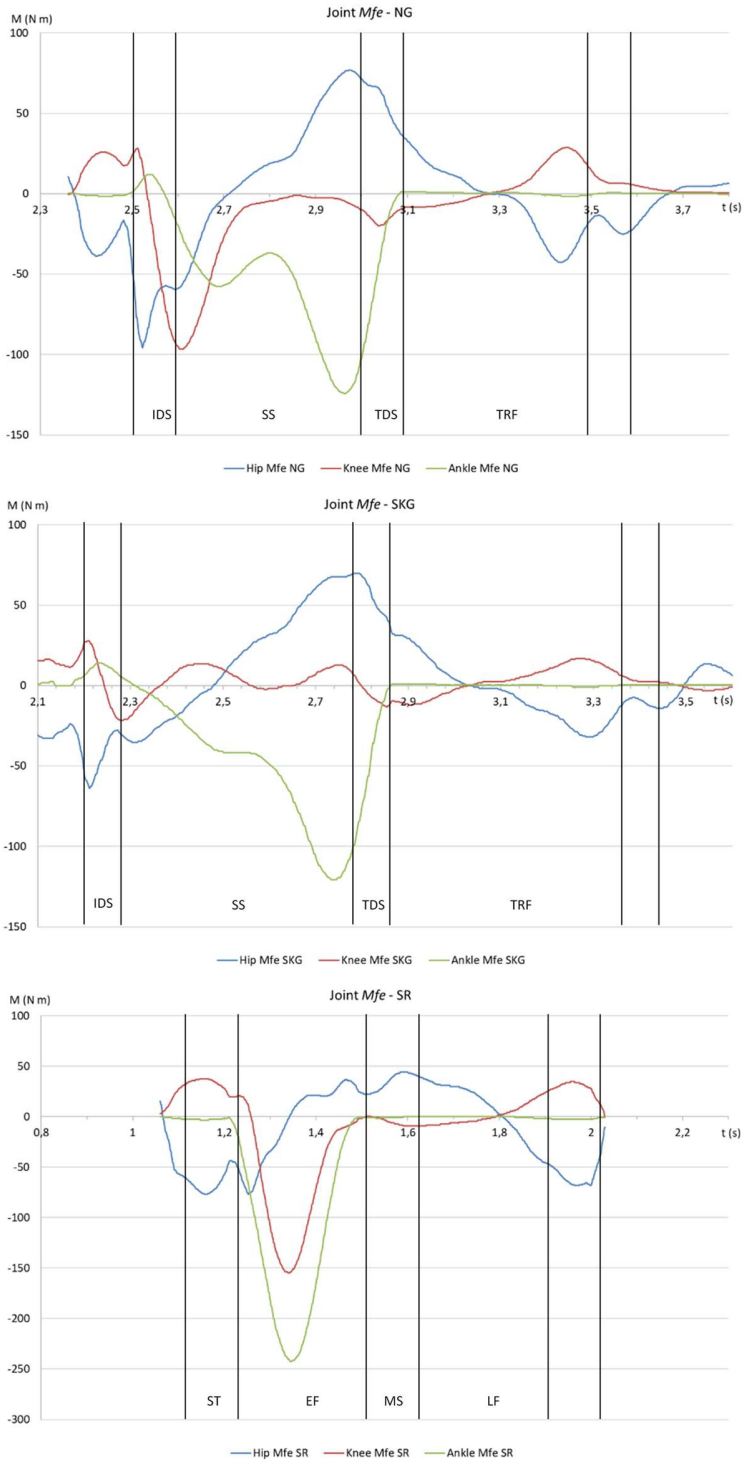

Fig. 8: Estimated time profile of vertical force at the right, left and both ankle joints during NG, SKG and SR.

2.2 Frequency analysis

2.2.1 Vertical ground reaction forces

Higher amplitude coefficients from Fourier series decomposition (1) of ground reaction force at the right foot Fz_1 were found, apart from continuous component with zero frequency, at the harmonics with 3.4 Hz and 5.1 Hz for NG, 3.0 Hz and 4.5 Hz for SKG and 3.6 Hz for SR, Fig. 9. 90% convergence of Fz_1 Fourier series was found at lower frequency 3.6 Hz for SR and higher frequencies 66.2 Hz for NG and 63.4 Hz for SKG. The amplitude of the harmonic with maximum value presents lower value at SKG than at NG and at NG than SR. Existence of higher number of harmonics with considerable amplitude and lower convergence rate of the Fourier series at NG and SKG than SR can be associated to shape differences at $Fz_1(t)$ with two relative maximum values at NG and SKG in contrast with one maximum at SR and the amplitudes of the harmonics with higher frequency at NG and SKG to the higher frequency oscillation of $Fz_1(t)$ at the start of IDS, Fig. 4.

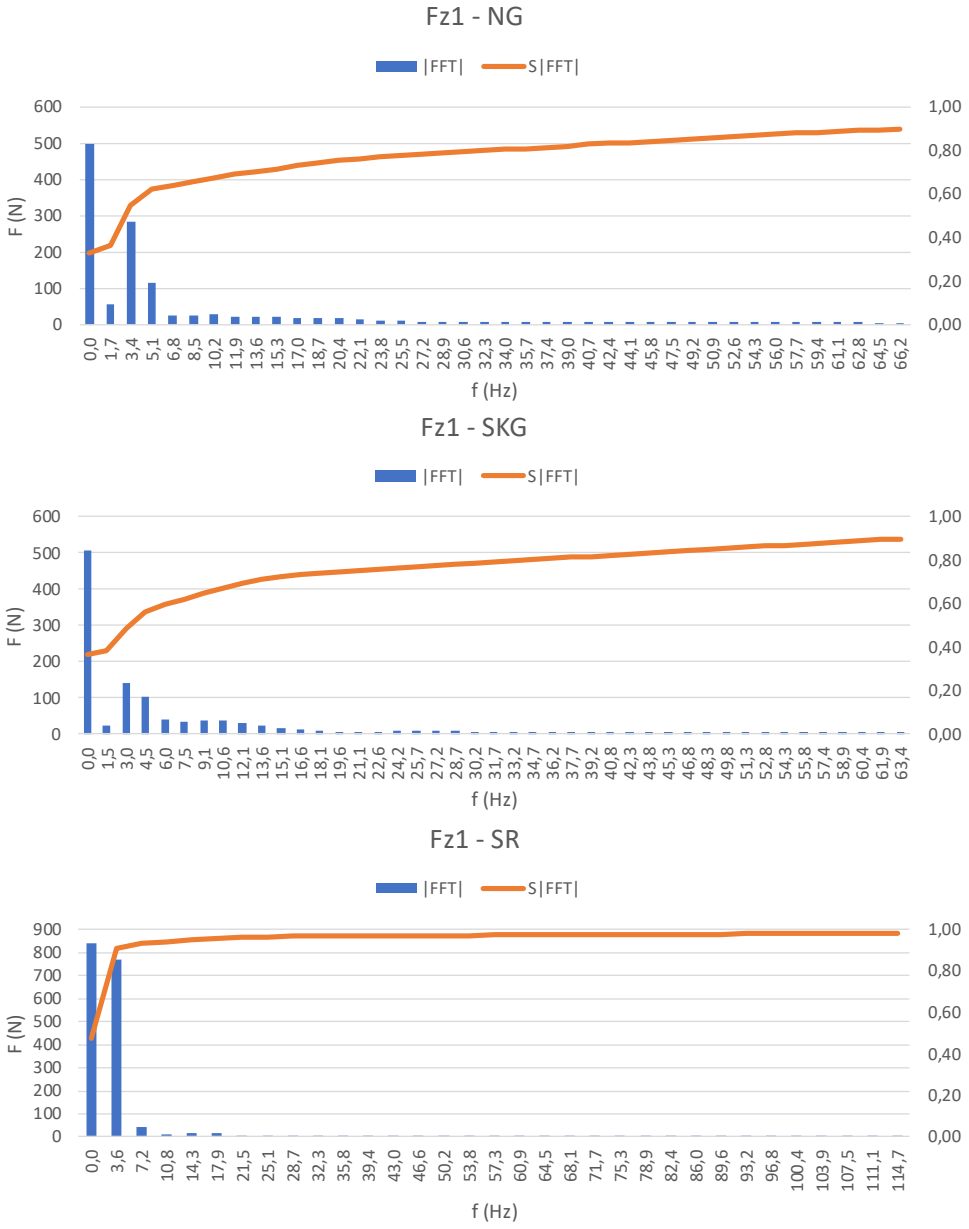

Fig. 9: Amplitude and accumulated relative frequency of coefficients from Fz_1 Fourier series decomposition during NG, SKG and SR.

2.2.2 Vertical joint forces

Separately the right and left sides present lower frequency of maximum FFT joint vertical forces *JFz* for the hip, knee and ankle than conjunct FFT decomposition of *JFz* at both sides, with the exception of *JFz* at the ankle presenting similar values of lower frequency FFT decomposition separately and conjunctly for NG, Fig. 10.

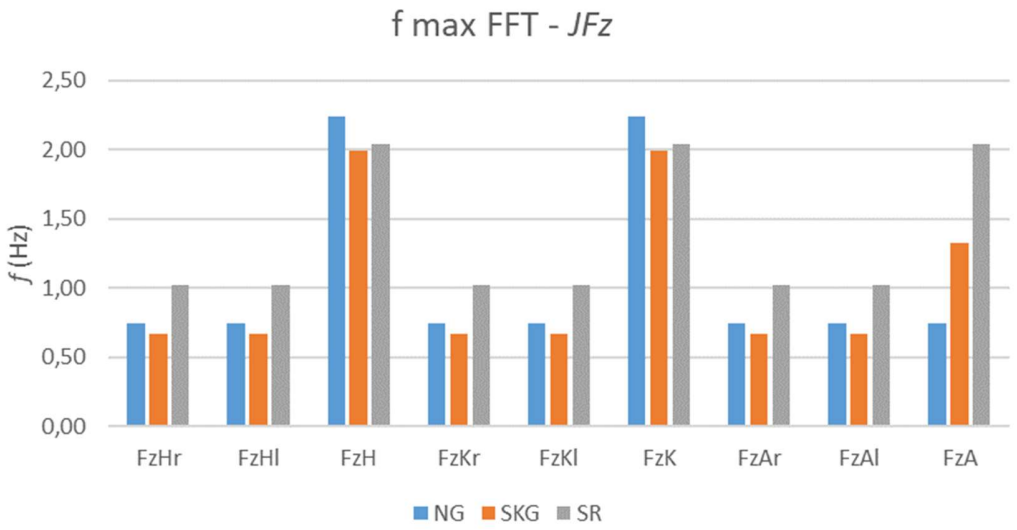

Fig. 10: Frequency of maximum amplitude coefficients from Fourier decomposition of *JFz* at the right (r), left (l) and both sides of the hip (H), knee (K) and ankle (A) during NG, SKG and SR.

90% convergence of the FFT amplitude from joint vertical forces *JFz* decomposition occurred at low frequencies for NG and SR than SKG for the hip, knee and the ankle with the exception of *JFz* at the left hip with SR presenting higher value than SKG and left ankle presenting higher value at NG than SKG, Fig. 11.

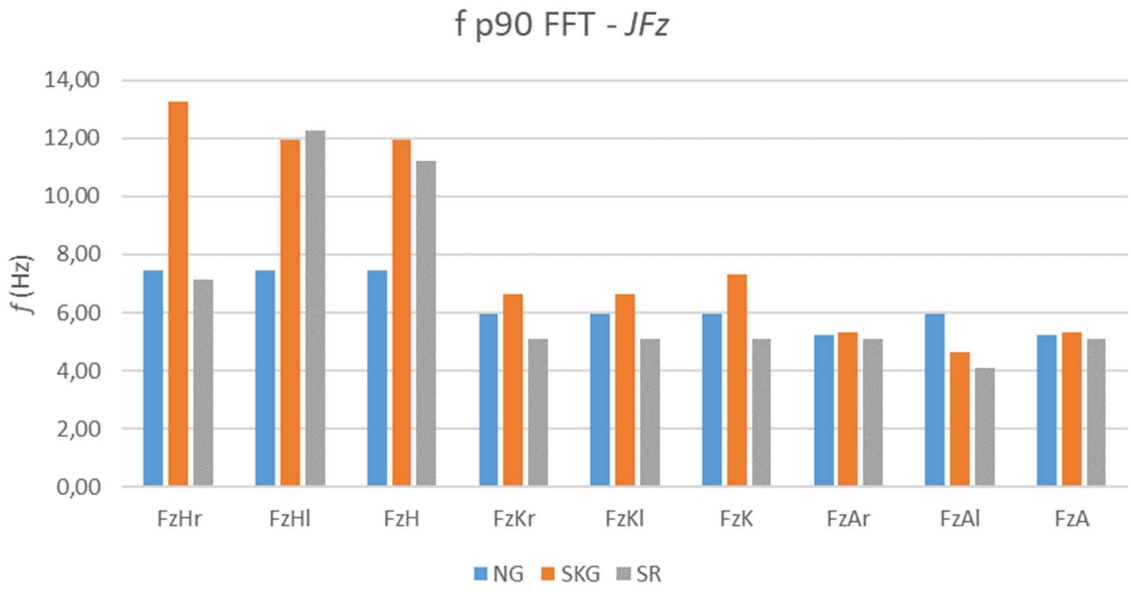

Fig. 11: Frequency of 90th amplitude coefficients from Fourier decomposition of *JFz* at the right (r), left (l) and both sides of the hip (H), knee (K) and ankle (A) during NG, SKG and SR.

2.2.3 Flexion-extension joint force moments

NG presented for the hip, knee and ankle lower frequency of the maximum amplitude values of *Mfe* FFT than SR, Fig. 12. SKG presented higher frequency of the maximum amplitude values of *Mfe* FFT at the knee and lower values for *Mfe* at the hip and the ankle in relation to NG and SR, Fig. 12.

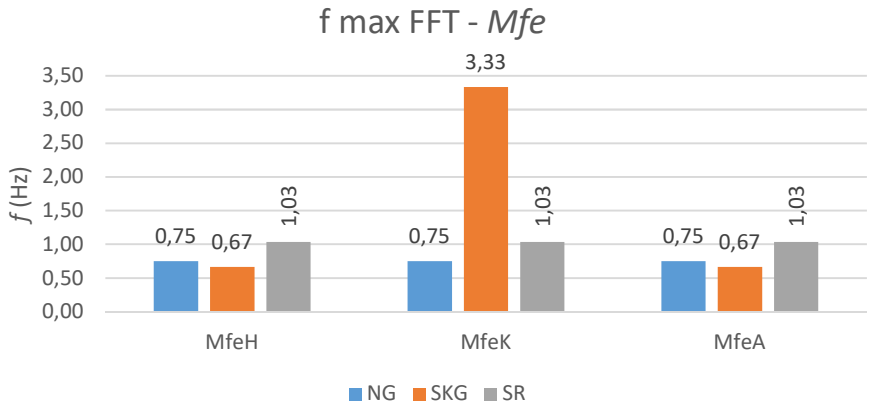

Fig. 12: Frequency of maximum amplitude coefficients from Fourier decomposition of *Mfe* at the hip (H), knee (K) and ankle (A) during NG, SKG and SR.

90% convergence of the FFT amplitude from Mfe decomposition, Fig. 13, were detected at similar low frequencies on NG, SKG and SR for the ankle with higher values at the knee in particular for SKG and at the hip for SKG and SR, Fig. 13.

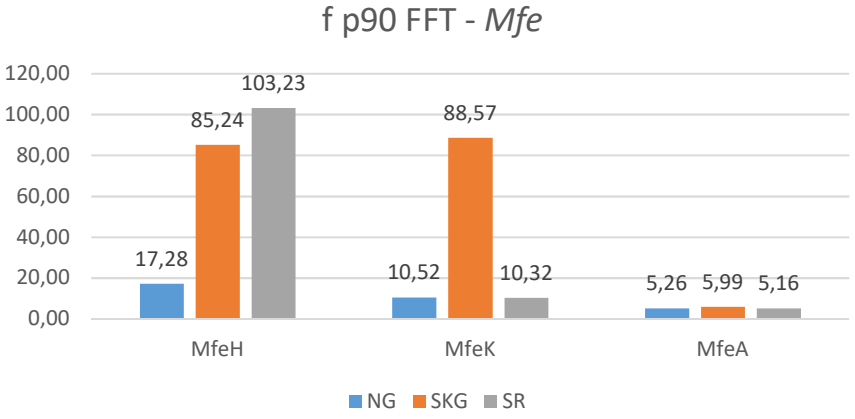

Fig. 13: Frequency of 90th amplitude coefficients from Fourier decomposition of *Mfe* at the hip (H), knee (K) and ankle (A) during NG, SKG and SR.

3 Discussion and conclusions

Most frequent analysis of ground reaction forces, joint contact forces and force moments are discrete time domain namely based on extreme, maximum and minimum values and their respective time of occurrence without taking into account overall pattern of data and the possibility of similar extreme values at different assessment conditions and undetected subtle graphs shape differences [4]. Present study extends proposed two term Fourier analysis of ground reaction forces during walking and running [10] to *GRFz*, *JFz* and *Mfe* for assessment of power spectrum distribution along subsequent harmonics, discriminating NG, SKG and SR at frequency domains.

According to this purpose, differences were detected on power spectrum at *GRFz* with higher power dispersion and lower amplitude of maximum FFT coefficients at SKG than NG and at NG than SR. SKG presented lower frequencies of maximum *JFz* FFT coefficients than NG at the right, left and both sides taken together for the hip, knee and ankle joints with exception of *JFz* ankle when both sides are considered together. SKG presented globally higher frequency of JFz FFT 90^{th} percentile in relation to NG and SR at the right, left and both sides of the hip, knee and ankle with the exception of left hip presenting higher frequency at SR and left ankle presenting higher value at NG. *Mfe* presented for the hip and the ankle lower frequency of maximum FFT coefficient at SKG than NG and at NG than SR. At the knee SKG presented higher frequency of the maximum *Mfe* FFT than SR and SR higher value than NG.

References

[1] J. Perry, and J.M. Burnfield, The functional structure of the lower limb. Gait Analysis: Normal and Pathological Function. Thorofare, NJ: SLACK Incorporated, 2 ed., 2010.

[2] G.J. van Ingen Schenau and A.J. van Soest, *On the Biomechanical Basis of Dexterity*. In: M.L. Latash,, M.T. Turvey, (eds.) Dexterity and its development, pp. 305–338. New Jersey, NJ: Lawrence Erlbaum Associates, Inc. Publishers, 1996

[3] A. Erdemir, S. McLean, W. Herzog, and A.J. van den Bogert, "Model-based estimation of muscle forces exerted during movements," *Clinical Biomechanics*, vol. 22, pp. 131–154, 2007.

[4] N. Stergiou, *Innovative Analyses of Human Movement*. Champaign, IL: Human Kinetics, 3 ed., 2004.

[5] J. Rasmussen, M. de Zee, and M.S. Andersen, *Assignment for the course in musculoskeletal modeling by multibody biomechanics*. Aalborg University, DK: Department of Mechanical and Manufacturing Engineering, 1 ed., 2012.

[6] M.D.K. Horsman, The Twente Lower Extremity Model: Consistent Dynamic Simulation of the Human Locomotor Apparatus. PhD thesis University of Twente: Netherlands, 2007.

[7] S. Hammer, C. Anderson, E. Guendelman, C. John, J. Reinbolt, and S. Delp, OpenSim Tutorial #3. Scaling, Inverse Kinematics, and Inverse Dynamics. Neuromuscular Biomechanics Laboratory: Stanford University, 2012.

[8] J. Rasmussen, M. Damsgaard, and M. Andersen, "Muscle recruitment by the min/max criterion – a comparative numerical study," *Journal of Biomechanics*, vol. 34, pp. 409–415, 2001.

[9] R. McN. Alexander, Optima for Animals. Princeton, NJ: Princeton University Press, 1996.

[10] R. McN. Alexander and A.S. Jayes, "Fourier analysis of forces exerted in walking and running," *Journal Biomechanics*, vol. 13, pp. 383–390, 1980.